Calculation of Quadrupole Coupling Constants: From Gas to Liquid *

Hanspeter Huber

Institute of Physical Chemistry, University of Basel, CH-4056 Basel, Switzerland

Z. Naturforsch. **49a**, 103–115 (1994); received July 23, 1993

Nuclear quadrupole coupling constants for D, ^{14}N and ^{17}O calculated with basis sets of high local quality are reviewed. It is confirmed that the concept of high local quality gives reliable results for many molecules in the gas phase. The calculations are extended to the condensed phase by combining quantum chemical calculations with molecular dynamics simulations. An excellent agreement with experiment is obtained for the deuterium coupling in liquid D_2O and a fair agreement for ^{17}O coupling in liquid $H_2{}^{17}O$. The ^{21}Ne nmr relaxation time in liquid neon is calculated to be within about 20% of experimental values, an exact comparison being difficult due to only roughly known pressures in the experiment and not adequately treated quantum effects in the simulations. Comparisons in the dense supercritical region at higher temperatures would be of interest, but experimental data are lacking.

Introduction

During the last decade several authors have contributed to progress in the determination of nuclear quadrupole moments by accurate calculations of electric field gradients (efg's) in small molecules [1]. Others, like our group, have made improved calculations on larger molecules where a compromise in the size of the basis set and the level of electron correlation has to be made [2–5]. As a logical extension we are heading towards the condensed phase, and the first results of couplings in liquid water [6–8] and neon [9] can be discussed.

Studies of D [2], ^7Li [3], ^{14}N [4] and ^{17}O [5] quadrupole couplings in single molecules showed that an improvement of previous work is possible if basis sets of high local quality at the nucleus of interest are used. The different mechanisms contributing to the efg. i.e. the distorted spherical orbitals in D and Li and the p-orbitals at N and O, mean that different levels of calculation should be applied. A large basis set is always needed, but in the first case SCF calculations yield a fair quality and one can use even simple models. In the second case, however, electron correlation should be included in the calculations. We will point out a model for D couplings [2] and a transformation problem [10], knowledge of which might be of some interest to the experimentalist.

In a second part, a new approach to calculate D [6, 7] and ^{17}O [8] couplings of liquid water will be discussed. In this, configurations of bulk water are produced in a molecular dynamics simulation. Clusters of a few water molecules are taken randomly from these configurations and used in super-molecule ab initio calculations to obtain the coupling of a nucleus in this cluster. The average of many such cluster calculations approaches the value of the coupling in the liquid. Temperature and pressure dependence were studied changing the conditions in the simulation. The results for deuterium are in excellent agreement with the most recent experiments, whereas for ^{17}O the calculated is roughly 10% larger than the experimental values.

A different, but also purely theoretical approach applied previously by Engström et al. [11] to aqueous solutions of alkali chlorides, was used to obtain the quadrupole coupling and spin-lattice relaxation time of neon in liquid and supercritical states. A comparison with experimental results in the liquid shows qualitative agreement, but a comparison at higher temperatures would be more interesting, as our classical simulations do not model quantum effects at low temperatures. However, experimental data in the supercritical region are lacking.

* Presented at the XIIth International Symposium on Nuclear Quadrupole Resonance, Zürich, July 19–23, 1993.

Reprint requests to Dr. H. Huber, Institut für Physikalische Chemie, Universität Basel, Klingelbergstrasse 80, CH-4056 Basel, Switzerland.

0932-0784 / 94 / 0100-0103 $ 01.30/0. – Please order a reprint rather than making your own copy.

Basis Sets of High Local Quality

Whereas efg's of small molecules can be calculated with very large basis sets including correlation, which leads, together with the experimental nuclear quadrupole coupling constants (QCC's) to some of the most accurate nuclear quadrupole moments [1], the costs for medium and large molecules are prohibitive. Figure 1 shows the calculated deuterium quadrupole coupling constant of DF on the SCF-level as a function of the basis set size. On this level the goal is to reach the Hartree-Fock limit of 344 kHz [12].

On the left, two points show the results with the most often applied double zeta (DZ) and douple zeta plus polarization (DZ + P) basis sets. Evidently, the results are far from acceptable. Two series of calculations to the right, one with a fixed DZ basis set and the second with an extended basis set on the F, show how large the basis set has to become until the results approach the Hartree-Fock limit. When electron correlation is included the basis should be still larger. However, such large basis sets are not feasible even for medium sized molecules. Therefore we introduced what we call "the concept of basis sets with high local quality".

Whereas normally one uses equal basis sets on equal atoms, we take a huge basis on the atom of interest, e.g. the deuterium, a large basis on the neighbour atom and only a double-zeta basis set on all atoms further away. Figure 2 shows for benzoic acid as an example a comparison between a DZ basis and the basis set we usually apply to calculate DQCC's.

The number of basis functions on each atom is shown as well as the total number for the example molecule. Our concept leads to quite large basis sets for small molecules but to a relatively small increase for larger molecules. We assume that the locally correct description of the electron distribution is most important for a correct description of the electric field gradient.

A question immediately arising is, whether such an "unbalanced" basis will introduce some unreal charge transfer and, hence, produce new artefacts rather than improved results. The answer can be given along three lines. Firstly, comparisons for many compounds and for different nuclei between calculated values obtained in this way and experimental couplings give an "empirical proof" that the approach works (see below). Secondly, a similar approach is taken all the time if the nuclei are not identical, i.e. for example in DF there is

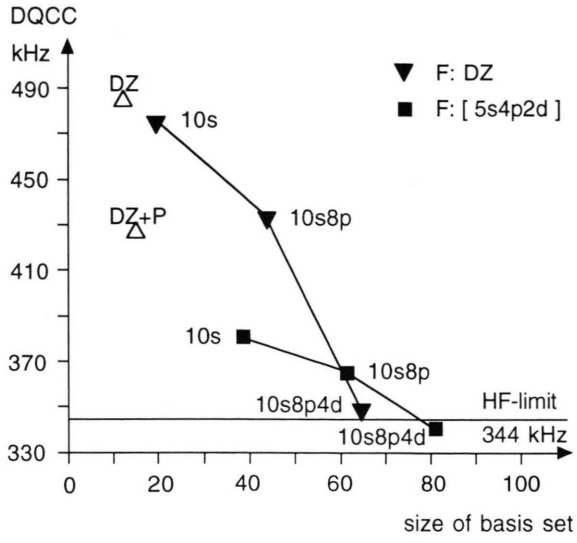

Fig. 1. Basis set dependence of the DQCC in DF on the SCF-level. The DZ and DZ + P basis sets yield couplings about 40% and 20% too large, respectively. Only very extended basis sets come close to the HF-limit.

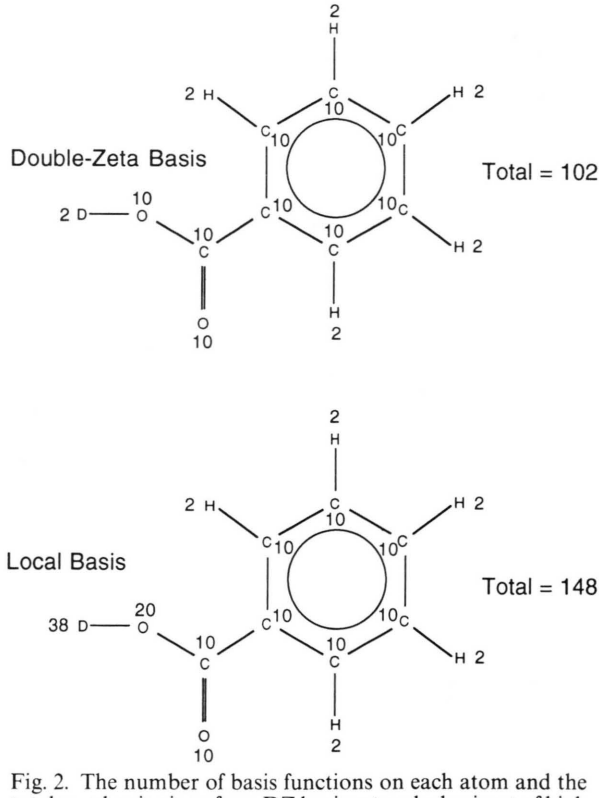

Fig. 2. The number of basis functions on each atom and the total number is given for a DZ basis set and a basis set of high local quality as applied in the calculations of the DQCC's given in this paper for benzoic acid as an example.

no way to say that a certain basis set for D may be used only with a certain basis set for F. Different combinations are possible, which could lead to similar unphysical charge transfers, but nobody cares in these cases. An example is the use of basis sets like 6-31G, 6-31G* and 6-31G**, with two double zeta (DZ) basis sets, a DZ on hydrogens and double zeta plus polarization (DZP) basis set on the other elements, and two DZP basis sets, respectively. Thirdly, a test calculation on H_2 with a normal (4s)/[2s] DZ basis set on one H and the large uncontracted 6s4p4d basis set on the other H shows a dipole moment of $0.046 \cdot 10^{-30}$ Cm only, corresponding to a transfer of 0.004 electrons (to the H with the smaller basis set).

Although, we have reasons to assume that this concept should be good for deuterium and still lead to an improvement for other nuclei, the final test is the comparison with experiment. Such comparisons are given in the next paragraph.

Nuclear Quadrupole Couplings in the Gasphase

The calculated coupling constants, obtained with basis sets of high local quality of most experimentally known DQCC's are plotted in Fig. 3 versus the experimental values [2].

Here, as well as in the calculations including electron correlation for other nuclei we used the nuclear quadrupole moment as a fit parameter to calibrate for defects in the calculation (limited basis set, limited inclusion of electron correlation, no vibrational correction). Only experimental values were used for the calibration, where the coupling as well as the structure (used in the calculation) were accurately known. With a few exceptions there is a good agreement which confirms the usefulness of this concept. The worst case was DNCO (triangle most to the right), which we had already calculated in 1985 on the SCF level to be far off the experimental value [13]. Because of the above discrepancy the coupling of DNCO has been remeasured in the meantime by Heineking et al. [14]. Whereas the predicted coupling constants were 286.3 kHz on the SCF-level and 277.0 kHz including correlation, the old experimental value was 345 ± 2 kHz and the new value is 285 ± 6 kHz, in good agreement with the calculations. This example shows that calculations, although they do not give such accurate values as experiment, can help in cases where the experimentalist has problems in the interpretation of the spectrum.

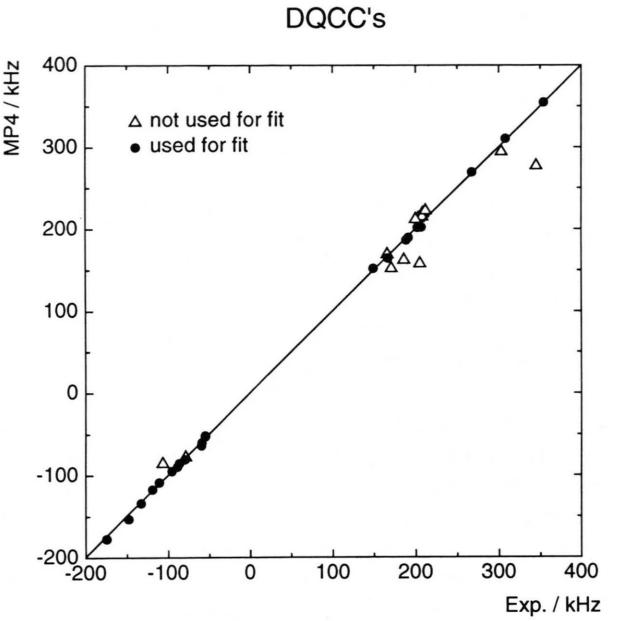

Fig. 3. Calculated (MP4(SDQ)) versus experimental DQCC's (all diagonal elements of the tensor were included, if not determined by symmetry). The nuclear quadrupole moment is used as a fit parameter.

However, it must be admitted that such cases are not very common. A more frequent problem where calculations can help are errors due to assumptions made for the transformation. Whereas the experimentalist often obtains only the diagonal elements of the coupling tensor in the principal axes of the moment of inertia, the quantum chemist obtains the full quadrupole coupling tensor and, therefore, has the possibility to transform the coupling tensor to any coordinate system.

Figure 4 shows the three coordinate systems of interest in this context for DNO_3 as an example.

The experimentalist obtains his data in the principal axes system of the moment of inertia. For comparison he would usually like to transform to the second one, the principal axes system of the DQCC, or to the third one, where one axis is along the bond. A problem arises if he does not know the off-diagonal components of the coupling tensor. Then it is often assumed that the angle α between the second and the third system, which is only a few degrees, may be set to zero. With this assumption a transformation without off-diagonal components is possible. It has always been assumed that the error introduced in this way would be small. Depending on the transformation angle φ,

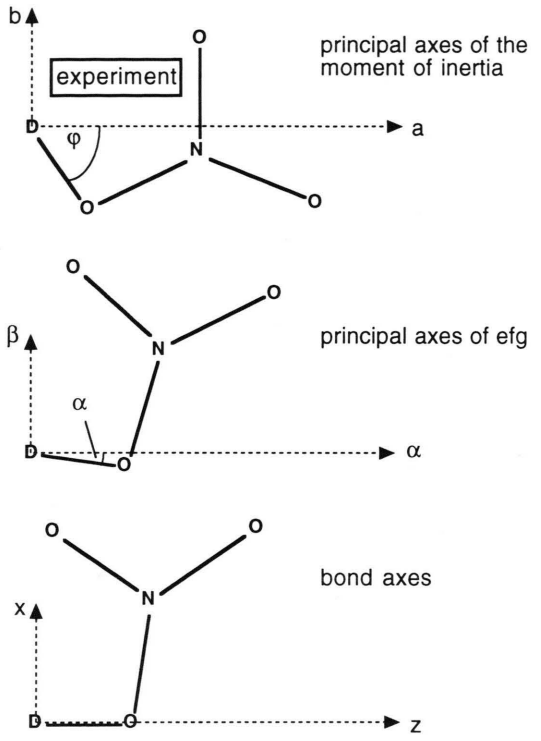

Fig. 4. Coordinate systems of interest. The second and third coincide if the usual assumption that α is zero is made for the transformation. The size of the angle φ is critical for the error introduced by the above assumption.

this might not be true at all. For planar molecules a linear error propagation yields for the error of the coupling constant $V_{\alpha\alpha}$ in the principal axes system of the coupling tensor [10].

$$\Delta V_{\alpha\alpha} = (V_{aa} - V_{bb}) \{\tan(2\varphi)/\cos(2\varphi)\} \alpha , \qquad (1)$$

where V_{aa} and V_{bb} are the two diagonal components of the coupling tensor in the experimental coordinate system in the plane of the molecule and α is in radians. If φ approaches 45°, $\tan(2\varphi)$ is going toward infinity and $\cos(2\varphi)$ toward zero, which yields an infinite error. This is illustrated for DNO_3 in Figure 5.

Although α is in this case only 1.07°, the assumption that it is zero yields an error of 16 kHz or 6%. Even a rough estimate of α would be better than this assumption. A still better way is to transform without the assumption and to use instead calculated off-diagonal elements.

Up to now two examples were given how calculations may help to find or reduce errors in the evaluation of experimental data. Another, and perhaps an

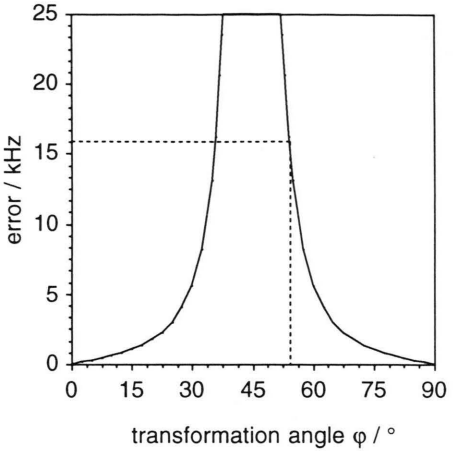

Fig. 5. Error in the DQCC of DNO_3 introduced by the assumption that α is zero (calculated $\alpha = -1.07°$, $V_{aa} - V_{bb} = -87.4$ kHz). The calculated transformation angle φ for DNO_3 is 54°.

even more appealing field, are model calculations which help to understand the underlying mechanisms. Calculations of "unreal" situations give the possibility to get insights which are not possible in experiment. For example, if the electric properties of a molecule change due to a substitution, this leads automatically to a different bond-length at the deuterium. It is easy to carry out the calculation at equal bond-lengths and hence find the individual contributions to the change of the coupling constant [15] due to the electric effects and the bond-length, respectively. Similarly, the calculated values can be divided into single orbital contributions leading to a better understanding.

Here we give a model which allows the prediction of DQCC's in a few minutes with the help of a desk calculator if the deuterium bond-length is known. It was published before incorrectly [2]. Other empirical relations have been published [16–20], but all of them were limited to certain classes of compounds. Quantum chemical calculations make it easy to obtain data for any class of compounds and hence to find a more general empirical model. Equation (2) is such a model which gives coupling constants along the bond with fair accuracy for all DQCC's (except for the simple molecules DH and DF [13]):

$$\mathrm{DQCC/kHz} = 1.9916 \cdot 10^8 \cdot \left\{ Z_v - 1.875 \right) \left(1 - \frac{1}{1 + 3.0126\,(\langle r \rangle / r)^5} \right) - 0.029\,\Delta \Big\} \cdot \frac{1}{(r/\mathrm{pm})^3} , \qquad (2)$$

where Z_v is the number of valence electrons and $\langle r \rangle$ the expectation value of the orbital radius (given in Table 1) of the neighbouring atom, respectively. Δ is the sum of the differences of Pauling's electronegativities between the second neighbours and the neighbour atom and r is the bond-length between the deuterium atom and its neighbour. The orbital radii for hybrids are taken as arithmetic means. The three numbers inside the brackets are fit parameters. For details see [2, 13].

To give an example, we apply (2) to DCOOH: $r = 109.1$ pm, $Z_v(C) = 4$, $\langle r \rangle_s (C) = 85$ pm, $\langle r \rangle_p (C) = 93$ pm, $\Delta = 2 \cdot (3.5 - 2.5) = 2$. $\langle r \rangle (C_{sp^2}) = (85 + 2 \cdot 93)/3$ pm $= 90.33$ pm, which yields DQCC(DCOOH) $= 167.0$ kHz in good agreement with the experimental value of 166 ± 2 kHz.

Figure 6 shows the values predicted with the model versus the calculated values.

The standard deviation is 7 kHz or about 4%. It is generally valid for DQCC's and, hence, can be used for a fast confirmation of a spectral interpretation. To find a similar model for the asymmetry parameter η is difficult, if not impossible. Calculations on a water monomer disturbed by a small point charge show that one can predict the direction in which η changes by calculating the field gradient due to the point charge only, but the size depends much on the deformation of the electron cloud (Sternheimer shielding), which can hardly be accounted for by a simple model.

Up to now we have mainly discussed DQCC's. However, the concept of basis sets with high local quality also improves calculations for other nuclei. Figures 7 and 8 show the calculated versus experimental QCC's for ^{14}N and ^{17}O, respectively. Whereas DQCC's are obtained reasonably accurate already on the SCF-level of theory, for these nuclei electron correlation should be included.

Figure 9 shows qualitatively the electric field gradient due to an electron in an s-orbital, and one component due to an electron in a p-orbital. With the help of this figure one can discuss the main differences in the mechanisms leading to the quadrupole couplings.

The electron in an s-orbital leads to a zero efg in a free deuterium atom. But, as can be seen from Fig. 9a, already small disturbances, e.g. a polarization moving the electron cloud away from the nucleus, leads to large field gradients. It is not so much a question whether the rest of the molecule withdraws electrons from the deuterium or vice versa, as this does not change the zero field gradient of a spherical charge

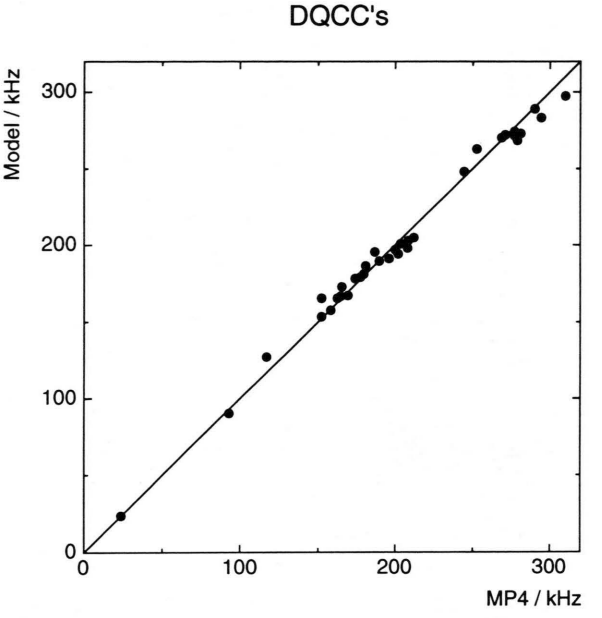

Fig. 6. DQCC's calculated with (2) versus the values obtained from the ab initio MP4(SDQ) calculations.

Table 1. Approximate orbital radii $\langle r \rangle$ (in pm)[a].

	Li	C	N	O	F	Na	Si	P	S	Cl
s-orbital	184	85	70	60	(53)	200	116	103	91	82
p-orbital	–	93	78	67	(58)	–	149	126	110	98

[a] for a discussion see [13].

distribution, but it is the polarization which is mainly due to the next neighbour and its distance which deforms the electron cloud and draws it away from the nucleus, and hence leads to the field gradient. This explains why it is possible to make models which predict the size of the coupling distance mainly on the basis of the bond-length. It might also be an explanation why DQCC's are calculated reasonably accurately already on an SCF-level. The structure and hence the important bond-length is usually taken from experiment and the SCF calculations give charge distributions accurately enough. However, enough basis functions are necessary on the deuterium atom as they have to model accurately the deformation of the electron cloud.

The situation is quite different for atoms with partially occupied p-orbitals. In this case there is a large efg already without any effects from the surrounding. Electric effects which might be due to groups quite far

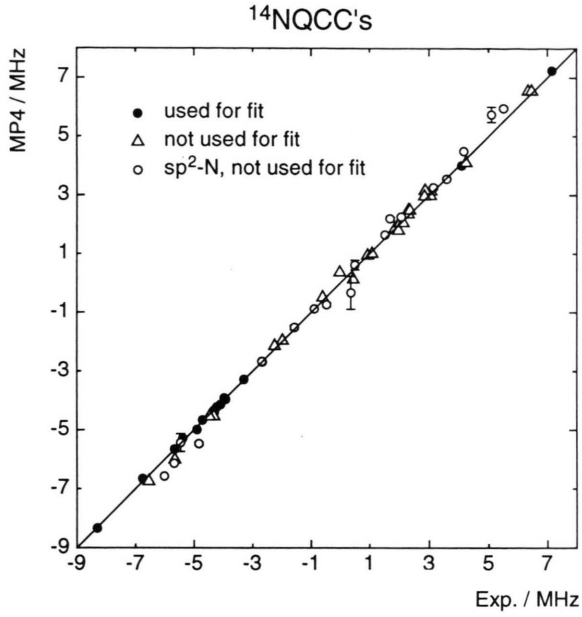

Fig. 7. Calculated (MP4(SDQ) versus experimental ^{14}NQCC's (all diagonal elements of the tensor were included, if not determined by symmetry). The nuclear quadrupole moment is used as a fit parameter. The calculated values for sp^2-hybridized nitrogens show worse agreement with experiment. Only in some cases this might be due to inaccurate experimental values (see experimental error bars given for these cases).

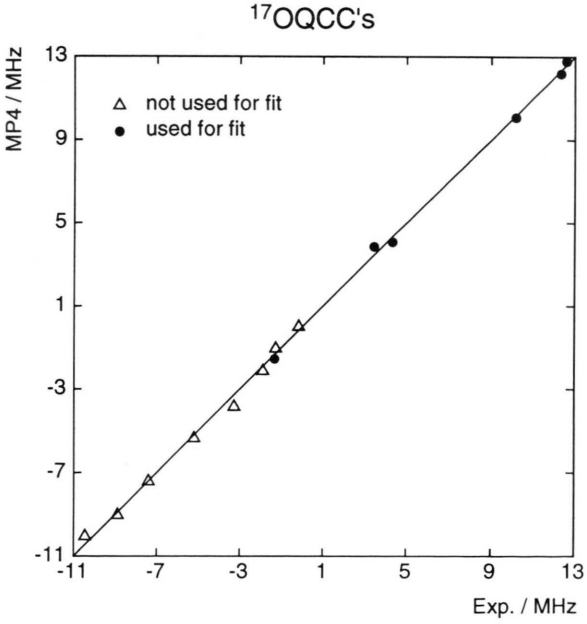

Fig. 8. Calculated (MP4(SDQ)) versus experimental ^{17}OQCC's (all diagonal elements of the tensor were included, if not determined by symmetry). The nuclear quadrupole moment is used as a fit parameter.

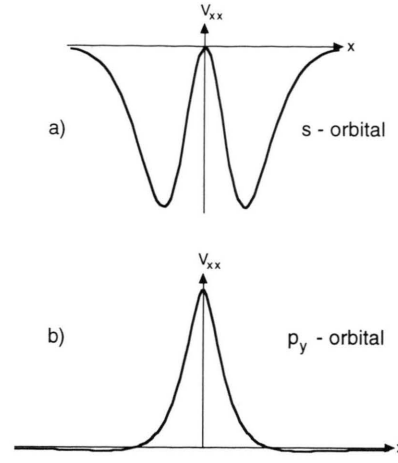

Fig. 9. Qualitative behaviour of the quadrupole coupling element V_{xx} induced by an electron a) in a s-orbital and b) in a p_y-orbital as a function of the distance along the x-axis.

Table 2. Origin of the efg at different nuclei.

	D	^{7}Li	^{14}N, ^{17}O, etc.
efg due to occupied p-orbital	–	–	0.5–2.0 a.u.
changes due to electronic surrounding	small	**small**[a]	**important**
bond-length to neighbours	**short**	long	unimportant
efg due to neighbour	**0.2–0.5 a.u.**	**small**[a]	unimportant

[a] 0.005–0.05 a.u.

away from the nucleus of interest change the charge in the p-orbital and have, therefore, a very direct influence on the size of the coupling. The structure and hence bond-length have only a minor influence. Electron correlation is of importance to describe accurately the electron distribution, which is the primary effect. To find a simple model for the efg would also mean to find one to describe the electron distribution in a molecule accurately, which is not very likely.

Table 2 gives a schematic overview over the situation. N and O stand for any nuclei with partially filled p-orbitals. Li is included as it is a boundary case. Due to the long bonds formed by lithium, the polarization effect is much smaller than in deuterium. Other electronic effects are of similar size, and an accurate calculation of these small effects (being differences of gradients due to the positive nuclei and negative electrons) is quite difficult.

Nuclear Quadrupole Couplings in the Liquid

a) DQCC of Liquid D_2O

To calculate NQCC's in the liquid phase one has to go beyond the quantum chemical calculation on a single molecule. Monte Carlo or molecular dynamics simulations can be used to study the quantitative behaviour of liquids. As our studies will sometimes include dynamical properties, we used molecular dynamics simulations.

A single water molecule as approximately observed in the gas phase shows a DQCC of 308 kHz, which is lowered in ice to a value between 200 and 220 kHz depending on the modification. This lowering is evidently due to the surrounding, mainly to the closest neighbours and their hydrogen bonds. Therefore the following approach should be successful.

In a molecular dynamics simulation of liquid water, snap-shots are taken from time to time. A deuterium is randomly chosen from each snap-shot and its nearest neighbours are evaluated, yielding clusters of water molecules with the chosen deuteriums in the center. Each cluster is used as a super-molecule in a quantum chemical calculation of the efg in the same way as in the gas phase. Each cluster corresponds to a typical surrounding of a water molecule in liquid water, and the average of many such calculations should then yield the liquid water value. Figure 10 compares calculated with experimental results at different temperatures. Details of the calculations were published previously [6, 7].

The calculated values for a distinct temperature were obtained as average from 82 ab initio calculations of clusters consisting of five water molecules, which were taken from simulations with 125 molecules applying an ab initio potential for water from Lie and Clementi [21], which is abbreviated in the following by LC. The statistical standard deviation for the coupling constant is about 5 kHz. The two experimental and the calculated series of couplings agree within the error limits, but the standard deviations are in all cases too large to show a significant temperature dependence. Before going into a more thorough discussion we will show now that a model for the coupling along the bond will improve the qualitative understanding as well as the quantitative results. Figure 11 shows two of the above mentioned 82 clusters, the left being the one with the smallest and the right the one with the largest coupling.

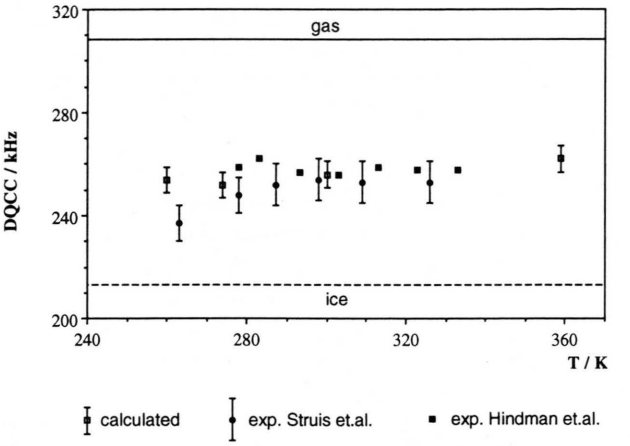

Fig. 10. Experimental and calculated DQCC's as a function of temperature in liquid D_2O. The error bars for the calculated values give only the statistical error.

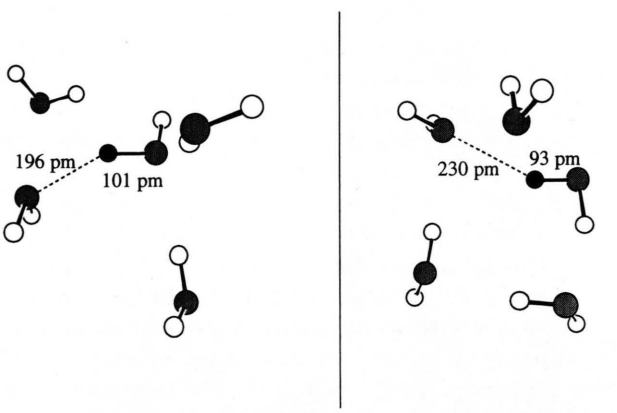

Fig. 11. The cluster with the smallest (left) and largest (right) DQCC in D_2O from the 82 samples taken from the molecular dynamics simulation.

The couplings can qualitatively be understood as we know that the DQCC is the larger, the shorter the bond-length, and is lowered by the hydrogen bond. Then the left one has a small coupling because the bond-length is very long (101 pm versus 95.7 pm in the gas), and the relatively short hydrogen bond decreases it further. The one on the right is large as it has a short bond-length (93 pm versus 95.7 pm in the gas) and is not much decreased by the long hydrogen bond. If this picture is correct it should be possible to make a simple two-term model which reproduces the main feature of the dependence of the coupling.

$$\mathrm{DQCC/kHz} = 2.20 \cdot 10^7 (r_{\mathrm{OD}}/\mathrm{pm} - 54.5)^{-3} - 2.06 \cdot 10^8 (r_{\mathrm{O}\ldots\mathrm{D}}/\mathrm{pm})^{-3}. \quad (3)$$

The equation shows a model with three parameters fitted at the 82 values calculated quantum chemically, which reproduces the 82 couplings with a standard error of 5.7 kHz or 2% error.

The model yields a gas phase value (not used in fitting) of 315 kHz compared to the ab initio value of 316 kHz. It also shows the right physical behaviour if the bond-lengths are increasing towards infinity. In contrast to similar models in the literature (see e.g. [20]), this model is fitted on non-equilibrium configurations.

A qualitative understanding of the mechanism leading to the coupling constant in the liquid is now obtained by applying the model to the 82 configurations from the simulation once with the hydrogen bridge bond-length set to infinity (i.e. only the left term in (3) is applied) yielding an "intramolecular" coupling of 280 kHz, and once with the OD-bond-length set to infinity (i.e. only the right term in (3) is applied) yielding an "intermolecular" contribution of −24 kHz. This means that 40% of the decrease is directly due to the influence of the hydrogen bridge, whereas 60% is due to the increase in the OD-bond-length (which in turn is again caused by the hydrogen bridge). How this model will improve the quantitative results will now be discussed with the help of Table 3.

This table gives the calculated coupling constants from Fig. 10. in the second column. The third column shows the corresponding couplings obtained with (3), applying it to the two deuteriums of each of 125 molecules in the 82 snap-shots. The huge number of 20 500 values ($2 \cdot 125 \cdot 82$) yields a very small statistical error, which allows it to make a definite statement about the temperature dependence. There is a small but significant positive temperature dependence, which is a new finding. A similar behaviour was found for the pressure dependence [7]. A further and more surprising finding is given in the last column of Table 3. The asymmetry parameter η, which is 0.145 in the corresponding calculation for a single molecule in the gas phase (experimental values of 0.135 and 0.138 have been published), and experimentally between 0.1 and 0.134 for different ice modifications, is outside the ice-gas range and significantly larger than the gas value. Hitherto neither an experimental nor a calculated value was available, and for simplicity it was usually assigned a value between the ice and the gas value. Calculations on the monomer with bond-lengths and an angle equal to the average values in liquid water show that about half of the increase can be rationalized by the change of the molecular structure. An additional calculation on the monomer disturbed by a small negative charge at the position of the oxygen lone-pair forming the hydrogen bridge shows a further increase of η.

Table 3. DQCC and η in liquid water at different temperatures.

T/K	DQCC/kHz SCF	DQCC/kHz Eq. (3)	η
260	254 ± 5	259.5 ± 0.3	0.169 ± 0.003
274	252 ± 5	260.5 ± 0.3	0.168 ± 0.003
300	256 ± 5	260.9 ± 0.3	0.164 ± 0.003
359	262 ± 5	263.4 ± 0.3	0.165 ± 0.003

As this approach was applied for the first time, it had to be tested thoroughly. A run with 216 instead of 125 molecules showed no significant difference. This was expected as the efg is a local property which should not be influenced much by long range effects. The cluster size was increased up to nine molecules, which again did not yield different results. Neither did different criteria for the determination of nearest neighbours. The most important effect to study was the influence of different potentials. In addition to the LC ab initio potential, two empirical potentials were used for tests. One was the DP potential by Dang and Pettitt [22] and the second the BJH potential by Bopp, Jancso and Heinzinger [23]. Although all three potentials reproduce the OD-bond-length in the gas phase correctly, which is of importance as the coupling constant is strongly dependent on this bond-length, these potentials give quite different results for different properties as is shown for the pair distribution function of the intermolecular O · · · D length in Figure 12.

The coupling constants and asymmetry parameters obtained with these potentials at two different temperatures are given in Table 4.

The third column, giving the averages of the quantum chemically calculated coupling constants, does not allow safe conclusions to be made, whereas the fourth column, with the values obtained with the model and the large sample, shows that the different potentials yield the same coupling constants for equal temperatures but significantly different values for different temperatures. In addition it is confirmed that the surprisingly large asymmetry parameter is not an artefact of the potential.

Finally, one can give a best estimate for the calculated coupling constant at 300 K making corrections for known systematic errors. The average of 261 kHz

from Table 4 is probably about 3% too large, as we know that the gas phase coupling calculated on the same level of approximation is 3% larger than the experimental value. The corrected value for the liquid is then 254 kHz in excellent agreement with the newest experimental values of Leyte and coworkers [24, 25] of 253 ± 6 kHz (298 K), 254 ± 8 kHz (298 K) and 253 ± 8 kHz (309 K) as well as with the older value of Hindman and coworkers [26] of 258.6 kHz. We cannot give an accurate error for our coupling constant but would estimate it to be of the same size as the above experimental errors, i.e. the agreement is that close by chance. The importance of the result is that it is obtained in a fully independent way from experiment.

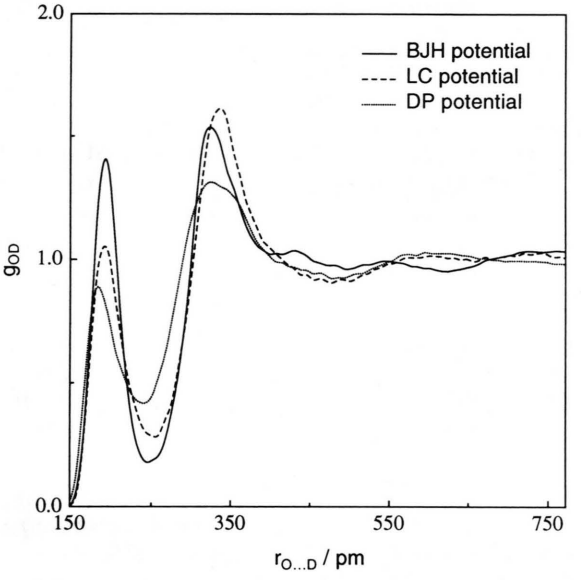

Fig. 12. The O · · · D pair distribution functions in liquid D_2O obtained with three different potentials (see text).

Table 4. DQCC and η in liquid water obtained with different potentials.

Potential	T/K	QCC/kHz SCF	QCC/kHz Eq. (3)	η
LC	300	256 ± 5	260.9 ± 0.3	0.164 ± 0.003
DP	303	263 ± 3	260.8 ± 0.2	0.172 ± 0.003
BJH	305	264 ± 6	261.1 ± 0.4	0.175 ± 0.004
LC	359	262 ± 5	263.4 ± 0.3	0.165 ± 0.003
DP	355	269 ± 3	264.7 ± 0.2	0.165 ± 0.003
BJH	363	266 ± 6	263.8 ± 0.4	0.172 ± 0.004

b) *^{17}OQCC of Liquid $H_2{}^{17}O$*

The same approach as for the DQCC was applied to the ^{17}OQCC in liquid water [8]. As the mechanism leading to the efg at ^{17}O is quite different than for deuterium, all the different tests like dependence on cluster size, on the potential etc. had to be repeated. We were not able to build a simple model for improving the statistics as was done for deuterium. The main results are given in Table 5.

A comparison between the first and second row shows that there is no significant difference for the two potentials. The same is true for the cluster sizes 5 and 9 as well as for the different temperatures. The asymmetry parameter η is close to the gas value but again outside the range given by the gas (calc. 0.8; exp. 0.75) and the ice (exp.: 0.865–0.97) value.

A best estimate for the coupling constant can be obtained as an average of the values given in the table, assuming that there is hardly any temperature dependence. This leads to a coupling constant of 8.9 MHz with an error probably not larger than about 0.3 MHz. This has to be compared with the experimental values of Hindman and coworkers [27] of 8.2 ± 0.2 MHz and of Leythe and coworkers [25] of 8.1 ± 0.4 MHz.

c) *Spin-Lattice Relaxation Time of ^{21}Ne in the Liquid and Supercritical State*

About three decades ago Henry and Norberg [28] showed that for liquid ^{21}Ne the quadrupolar relaxation mechanism is dominant. Due to its spherical symmetry there is no electric field gradient at the nu-

T/K	Potential	Cluster size	QCC_{aa}/MHz	QCC_{bb}/MHz	QCC_{cc}/MHz	η
300	DP	5	-7.92 ± 0.11	-1.15 ± 0.11	9.07 ± 0.10	0.749 ± 0.024
	LC	5	-7.95 ± 0.11	-0.93 ± 0.11	8.88 ± 0.10	0.795 ± 0.025
		9	-7.84 ± 0.10	-0.92 ± 0.11	8.76 ± 0.09	0.794 ± 0.024
360	LC	5	-8.04 ± 0.10	-0.97 ± 0.11	9.01 ± 0.09	0.789 ± 0.024
		9	-7.99 ± 0.11	-0.96 ± 0.11	8.90 ± 0.08	0.787 ± 0.024

Table 5. ^{17}OQCC and η in liquid water for different temperatures, potentials and cluster sizes.

cleus of a free neon atom, but in the liquid or supercritical phase the dynamics of the neighbour atoms induces a fluctuating electric field gradient. Together with the nuclear quadrupole moment of ^{21}Ne this leads to a fluctuating nuclear quadrupole coupling and hence to spin-lattice relaxation. Under extreme narrowing conditions the spin-lattice relaxation time T_1 is obtained from equation [29]

$$\frac{1}{T_1} = \frac{3}{8} \frac{2I+3}{I^2(2I-1)} \left(\frac{eQ}{\hbar}\right)^2 \langle V(0)\, V(0)\rangle \tau_{\text{eff}}\,, \quad (4)$$

where $I = \frac{3}{2}$ is the spin of ^{21}Ne, Q is the nuclear quadrupole moment of ^{21}Ne and τ_{eff}, an effective correlation time is given by

$$\tau_{\text{eff}} = \int_0^\infty \langle V(0)\, V(t)\rangle / \langle V(0)\, V(0)\rangle \, \mathrm{d}t\,, \quad (5)$$

with $\langle V(0)\, V(t)\rangle$ being the time correlation function of the field gradient in a laboratory coordinate system. The greater the coupling and the longer the effective correlation time, the shorter is the relaxation time. The necessary data can be obtained from molecular dynamics simulations as follows.

At each step of a molecular dynamics simulation the quadrupole coupling V is calculated and used to obtain its corresponding time correlation function $\langle V(0)\, V(t)\rangle$. This yields the average square value needed in (4) and the effective correlation time. However, had this to be achieved by quantum chemical calculations of clusters from snapshots as in the above case of water this would lead to excessive use of computer time. Therefore we use an approximation applied previously by Engström and coworkers [11, 29, 30] in the calculation of aqueous solutions of alkali chlorides. Similarly to the pair approximation for the potential energy, a pair approximation for the electric field gradient is used. The field gradient curve as a function of the dimer bond-length is obtained from a fit to points calculated with ab initio calculations including correlation:

$$q/\text{a.u.} = -26.19 \exp(-0.03156\, r/\text{pm}) - 4.083 \exp(-0.00008186\, (r/\text{pm})^2)\,. \quad (6)$$

To convert the electric field gradient in atomic units to a quadrupole coupling constant in MHz a conversion factor of 23.86 MHz/a.u. is applied, which is based on a quadrupole moment for ^{21}Ne of $10.155 \cdot 10^{-30}$ m^2 [31]. The field gradient for a nucleus is then calculated at each time step of the simulation in the two-particle approximation, evaluating (6) for all its neighbours, transforming to a laboratory coordinate system and summing up. Details of the calculations are reported in [9].

Relaxation Time (s)

T / K	ρ = 52509	56620	60731 mol m^{-3}
25	28.1	24.3	19.5
28	27.9	23.9	19.4
33	26.7	23.2	19.0

Fig. 13. Calculated ^{21}Ne relaxation times in liquid neon as a function of density and temperature.

^{21}Ne-QCC (kHz)
(absolute value)

T / K	ρ = 52509	56620	60731 mol m^{-3}
25	76.2	80.1	85.3
28	80.8	85.6	90.5
33	88.6	92.5	99.0

Fig. 14. Calculated ^{21}Ne quadrupole coupling constants in liquid neon as a function of density and temperature.

Figure 13 shows the spin-lattice relaxation times calculated for a grid of three densities and three temperatures. The arrows show the strong dependence on density and the surprisingly small dependence on temperature. They can be rationalized with the help of the quadrupole coupling and effective correlation time obtained independently in the simulations. Figures 14 and 15 show the same grid for these two properties.

The quadrupole coupling is strongly dependent on the density as well as on the temperature. The former can be explained with the smaller distances between the atoms hence inducing larger field gradients. The temperature dependence is due to the higher or lower energy collisions leading to shorter or longer collision distances and hence to different induced field gradients.

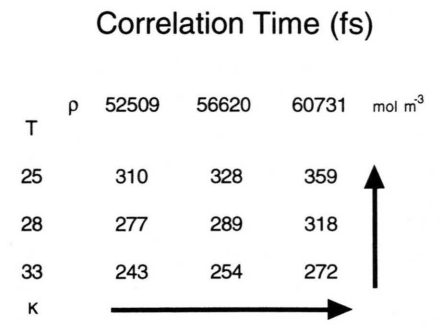

Fig. 15. Calculated correlation times in liquid neon as a function of density and temperature.

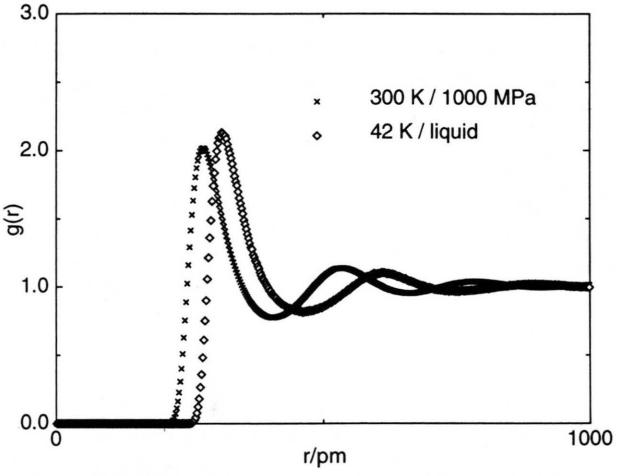

Fig. 16. Calculated Ne–Ne pair distribution function at a liquid and a supercritical state point of similar density.

Table 6. Comparison between a liquid and a supercritical state point of similar density of neon.

T/K	ϱ (mol m^{-3})	P_{sim} MPa	T_1 s	τ_{eff} fs	QCC kHz
33	60731	38.5	19.0	272	−99.0
300	59367	536	7.0	66	−332

The corresponding diagram for the effective correlation times in Fig. 15 shows the same dependence on density as the coupling, but an opposite temperature dependence. At higher densities it is more difficult for the neighbours to get away, hence leading to a longer correlation time. At higher temperature all movements are faster and therefore the correlation time decreases.

Combining the two opposite temperature dependences of the coupling and the correlation time leads to the surprisingly small temperature dependence of the relaxation time.

Table 6 makes a comparison between a state point in the liquid and in the supercritical region. They were selected to have similar density, and one might assume that they can be described by the same mechanical picture and having a similar structure, in one case at high, and in the other at low temperature and pressure.

Figure 16 shows the pair distribution functions for two similar state points in the liquid and supercritical phase, which indeed are about equal except for a radial shift. Whereas the curve for the liquid state point has its first maximum just about at the minimum of the potential well ($\approx$310 pm), the curve for the point in the supercritical region has its first maximum shifted by about 40 pm to a shorter distance where the potential curve shows a steep wall. Whereas the liquid shell structure is due to the small kinetic energy which does not allow the atoms to move out of the potential well easily, the supercritical shell structure is due to the high pressure which forces the atoms to fill the space and hence to form a shell around the atom. This immediately has its consequences for the relaxation time, as the smaller shell radius in the supercritical state leads to a much larger value for the coupling (intensified by the high energy collisions at the higher temperature), whereas the higher temperature shortens the correlation time as is shown by the numbers in Table 6.

Finally, we might ask how good these relaxation rates, which were obtained in a purely theoretical way, agree with experimental values. Unfortunately, no experimental data exist in the supercritical region, where a comparison would be more interesting, as quantum effects which are not included in the classical molecular dynamics scheme applied here are absent. The only comparison that can be made is with the data of Henry and Norberg [28] who, however, do not give the exact pressures in their experiments. Depending on the comparison (extrapolation to low pressures, applying quantum corrections) the deviation of the calculated from the experimental relaxation times is up to 20%.

d) Different Approaches for the Calculation of NQCC in the Liquid Phase

In principle the calculation of NQCC's in the condensed phase is straightforward. In a molecular dy-

namics simulation one has to calculate the efg quantum chemically in each step and to use it for the evaluation of the corresponding time correlation function. However, this at the moment is hardly feasible. The most natural scheme to perform such calculations in the near future might be to integrate it in a first principle molecular dynamics simulation [32].

At the moment several compromises are possible. If the time dependence is not needed, the approach with quantum chemical calculations for clusters taken from snap-shots of the simulation, as applied for the first time in the water couplings, are probably the best way. If the time dependence is needed as for the calculation of relaxation times, the approach with the two-particle field gradient curve, as first applied by Engström and coworkers and used here to neon, might be feasible. However, one has to be aware that for molecules one has to calculate a multidimensional efg surface, which means a high expense in computer time, if not obtained simultaneously with the potential surface. A cheaper but more approximate way has been used by Schnitker and Geiger [33] for xenon in water. They approximated the charge distribution of the water molecules with a few point charges and used these in the simulation to calculate the efg at the xenon nucleus due to these point charges. These are the only three approaches described in the literature as far as we are aware.

Conclusions

Experiments in the gas phase are still more accurate for medium or large size molecules than calculations. However, it was shown that the latter can be helpful to find errors in the interpretation of spectra and in the transformation from experimental to other coordinate systems. In the liquid phase, where experimental data are less accurate and assumptions have to made for the data-evaluation, calculations could become an accurate independent source of information, as is shown here for the D- and the ^{17}O-nuclear coupling constant in liquid water. However, the real value of calculations in both cases lies in the additional insights they can give into the mechanisms. For example the temperature independence of the relaxation time in liquid ^{21}Ne is shown to be the result of opposite temperature dependences for the quadrupole coupling and the effective correlation time.

Future work is planned to investigate computationally the surprising behaviour of the deuterium coupling of water in a water-DMSO mixture found by Gordalla and Zeidler [34] and the temperature behaviour of the deuterium coupling as well in the above mixture [35] as in liquid methanol [36].

Acknowledgement

This work is part of the Project 20-32284.91 of the Schweizerischer Nationalfonds zur Förderung der Wissenschaften.

[1] P. Pyykkö, Z. Naturforsch. **47a,** 189 (1992).
[2] S. Gerber and H. Huber, J. Mol. Spectrosc. **134,** 168 (1989).
[3] S. Gerber and H. Huber, J. Phys. Chem. **93,** 545 (1989).
[4] S. Gerber and H. Huber, Chem. Phys. **134,** 279 (1989).
[5] R. Eggenberger, S. Gerber, H. Huber, D. Searles, and M. Welker, J. Mol. Spectrosc. **151,** 474 (1992).
[6] R. Eggenberger, S. Gerber, H. Huber, D. Searles, and M. Welker, J. Chem. Phys. **97,** 5898 (1992).
[7] R. Eggenberger, S. Gerber, H. Huber, D. Searles, and M. Welker, J. Comput. Chem. accepted for publication.
[8] R. Eggenberger, S. Gerber, H. Huber, D. Searles, and M. Welker, Mol. Phys. in press.
[9] R. Eggenberger, S. Gerber, H. Huber, and M. Welker, Chem. Phys. accepted for publication.
[10] E. Fliege, H. Dreizler, S. Gerber, and H. Huber, J. Mol. Spectrosc. **137,** 24 (1989).
[11] S. Engström, B. Jönsson, and R. W. Impey, J. Chem. Phys. **80,** 5481 (1984).
[12] L. Laaksonen, P. Pyykkö, and D. Sundholm, Computer Physics Reports **4,** 313 (1986).
[13] H. Huber, J. Chem. Phys. **83,** 4591 (1985).
[14] N. Heineking, M. C. L. Gerry, and H. Dreizler, Z. Naturforsch. **44a,** 577 (1989).
[15] S. Gerber and H. Huber, J. Mol. Spectrosc. **138,** 315 (1989).
[16] L. Salem, J. Phys. Chem. **38,** 1227 (1963).
[17] M. Mokkarram and J. L. Ragle, J. Phys. Chem. **59,** 2770 (1973).
[18] M. Rinné and J. Depireux, Advances in Nuclear Quadrupole Resonance, ed. by J. A. Smith (Heyden, London 1974), pp 357ff.
[19] G. Soda and T. Chiba, J. Chem. Phys. **50,** 439 (1969).
[20] P. L. Olympia Jr., and B. M. Fung, J. Chem. Phys. **51,** 2976 (1969).
[21] G. C. Lie and E. Clementi, Phys. Rev. A **33,** 2679 (1986).
[22] L. X. Dang and B. M. Pettitt, J. Phys. Chem. **91,** 3349 (1987).
[23] P. Bopp, G. Jancsó, and K. Heinzinger, Chem. Phys. Lett. **98,** 129 (1983).
[24] J. R. C. van der Maarel, D. Lankhorst, J. de Bleijser, and J. C. Leyte, Chem. Phys. Lett. **122,** 541 (1985).
[25] R. P. W. J. Struis, J. de Bleijser, and J. C. Leyte, J. Phys. Chem. **91,** 1639 (1987).

[26] J. C. Hindman, A. J. Zielen, A. Svirmickas, and M. Wood, J. Chem. Phys. **54,** 621 (1971).
[27] J. C. Hindman, A. Svirmickas, and M. Wood, J. Phys. Chem. **74,** 1266 (1970).
[28] R. Henry and R. E. Norberg, Phys. Rev. B **6,** 1645 (1972).
[29] S. Engström, B. Jönsson, and B. Jönsson, J. Magn. Res. **50,** 1 (1982).
[30] S. Engström and B. Jönsson, Mol. Phys. **43,** 1235 (1981).
[31] D. Sundholm and J. Olsen, J. Phys. Chem. **96,** 627 (1992).
[32] R. Car and M. Parrinello, Phys. Rev. Lett. **55,** 2471 (1985).
[33] J. Schnitker and A. Geiger, Phys. Chem. N. F. **155,** 29 (1987).
[34] B. C. Gordalla and M. D. Zeidler, Mol. Phys. **59,** 817 (1986).
[35] B. C. Gordalla and M. D. Zeidler, Mol. Phys. **74,** 975 (1991).
[36] R. Ludwig, D. S. Gill, and M. D. Zeidler, Z. Naturforsch. **46a,** 89 (1991).